www.czasopisma.pan.pl PAN POLSKA AKADEMIA NAUK www.journals.pan.pl

Arch. Metall. Mater. **62** (2017), 2, 587-593

DOI: 10.1515/amm-2017-0087

A. SZCZOTOK*#, J. NAWROCKI**, J. PIETRASZEK***

THE IMPACT OF THE THICKNESS OF THE CERAMIC SHELL MOULD ON THE ($\gamma + \gamma'$) EUTECTIC IN THE IN713C SUPERALLOY AIRFOIL BLADE CASTING

In the study the wall thickness of ceramic shell mould influence on ($\gamma + \gamma'$) eutectic in the IN713C nickel-based superalloy airfoil blade casting was described.

Two castings formed as a blade from two wax pattern assemblies were analysed. In the experiment in one pattern the thick ceramic layer was obtained on pressure side and in another one on suction side of the airfoil blade. The microstructure of the cross-sections of the castings were observed on polished and etched metallographic specimens. The microstructure and phases chemical compositions of specimens was analyzed by using the scanning electron microscope Hitachi S-4200 equipped with EDS. It was established, that wall thickness of ceramic shell mould affect size, shape and volume fraction of ($\gamma + \gamma'$) eutectic islands in airfoil blade made from IN713C superalloy.

The analysis was provided in accordance to the typical statistical methodology [1].

Keywords: Investment Casting, IN713C Superalloy, ($\gamma + \gamma'$) Eutectic, Computing Methods, Statistical Analysis, Repeatability of Results

1. Introduction

Nickel-based superalloys are mainly used in aircraft and power-generation turbines. Creep-resistant polycrystalline turbine blades applied in the mentioned industry are typically produced by investment casting process also known as the lost wax process. It is especially useful for making castings of complex and near-net shape geometry, where machining may not be possible or too wasteful. The lost wax process is a complex, multi-step and relatively expensive manufacturing process, but allows to obtain the casting of such complex part with very thin section as the turbine blade with good surface finish and high dimensional accuracy. In the investment casting process a wax pattern (wax replica of the same basic geometrical shape as the intended finished cast part, prepared by injection into special, carefully calculated and manufactured wax die) is coated with a refractory ceramic material. Once the ceramic material has dried (hardened) its internal geometry takes the shape of the casting. The entire assembly is placed in a steam autoclave to remove most of the wax. The remaining amount of wax soaked into the ceramic shell is burned out in a furnace. The molten nickel-based superalloy is poured into the cavity where the wax pattern was. The metallic material solidifies within the ceramic shell mould. Once the casting has cooled sufficiently, the mold shell is broken out. Next, the gates and runners are cut from the casting. After minor final post processing (sandblasting, machining), the castings – identical to the original wax patterns – are complete and ready [2-6]. It is well known that many process parameters may influence on the quality of the final part, its microstructure and finally its properties.

2. Material for the research

Studies were performed on the IN713C superalloy, which besides nickel also contained (wt. %): 0.10% C, 13.5% Cr, 4.5% Mo, 6% Al, 0.8% Ti, 2% Nb, 0.01% B, and 0.06% Zr.

Polycrystalline nickel-based superalloys develop high temperature strength through solid solution and precipitation strengthening (the formation of secondary phase precipitates such as gamma prime and carbides). The microstructure of the IN713C consists, regardless of the casting parameters used, of γ-grains, carbides, interdendritic ($\gamma + \gamma'$) eutectic, (γ + MC) eutectic and coherent γ' precipitates distributed uniformly within the γ-matrix. The precipitation and growth kinetics of the γ' phase are highly sensitive to the rate at which the alloy is cooled through the solvus temperature.

The ($\gamma + \gamma'$) eutectic is an indication of the remaining melt at the end of the solidification process [7]. After solution heat treatment the microstructure with ($\gamma + \gamma'$) eutectic should be homogenized [8].

* SILESIAN UNIVERSITY OF TECHNOLOGY, FACULTY OF MATERIALS ENGINEERING AND METALLURGY, 8 KRASIŃSKIEGO STR., 40-019 KATOWICE, POLAND
** RZESZOW UNIVERSITY OF TECHNOLOGY, RESEARCH AND DEVELOPMENT LABORATORY FOR AEROSPACE MATERIALS, 12 POWSTAŃCÓW WARSZAWY AV., 35-959 RZESZÓW, POLAND
*** CRACOW UNIVERSITY OF TECHNOLOGY, FACULTY OF MECHANICAL ENGINEERING, DEPARTMENT OF SOFTWARE ENGINEERING AND APPLIED STATISTICS, 37 JANA PAWŁA II AV., 31-864 KRAKÓW, POLAND

Corresponding author: agnieszka.szczotok@polsl.pl

3. Methods

The castings described in the work were produced by the Laboratory for Aerospace Materials at Rzeszow University of Technology in Poland. The Laboratory carries on experiments among other things in the fields of innovation in foundry engineering. The polycrystalline castings from IN 713C were made in the investment casting process. Finding a correlation between the wall thickness of the ceramic shell mould and the as-cast microstructure (especially $(\gamma + \gamma')$ eutectic) of the castings from the IN713C was the main objective of the present study. Specific knowledge about conditions and parameters of the process is protected and therefore will not be discussed in detail. Two wax pattern assemblies (single wax blade replicas assembled in clusters) were prepared to produce several casts in a single casting. Each assembly consisted of two casts: one "smaller" airfoil blade casting and one "bigger" solid airfoil blade (see Fig. 1). Two castings: GK and GG (one from each assembly) were selected for the microstructural and statistical analysis (see Fig. 1).

Water-based colloidal silica slurry with different grain size of alumino-silicates filler and stucco were used to shell mould manufacturing. Each shell mould consisted of nine layers.

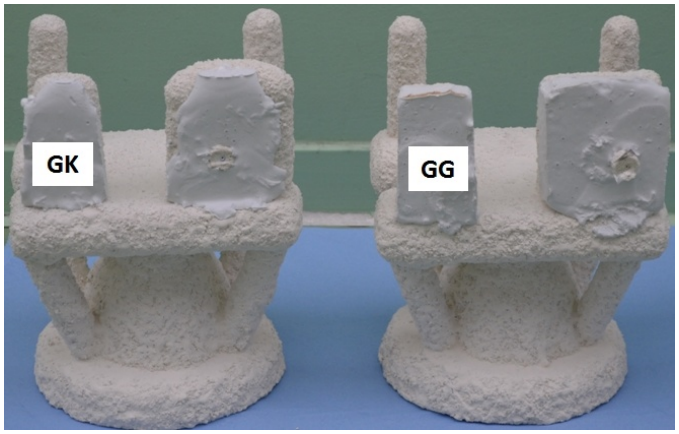

Fig. 1. Pattern assemblies with castings

Additionally, in the case of the GK casting from the first assembly, a thicker ceramic layer consisting of alumina (Al_2O_3) and silica (SiO_2) suspension in water mixed in proportion 2:1 was put on the suction side of the airfoil blade (see Figs. 2 and 3). The thickness of the ceramic shell mold wall was there 21÷24 mm. Whereas, the GG cast from the second assembly got extra thicker ceramic layer on the pressure side of the airfoil blade (see Fig. 3). The thickness of the ceramic shell mold wall was there 19÷24 mm.

The dry time to full shell production amounted to 24 hours. After dewaxing, the ceramic molds were placed in the furnace for vacuum casting and annealed up to 1200°C to build up their strength and make them ready to pouring with the molten IN713 superalloy at the temperature 1500°C. After pouring with liquid metal, the ceramic moulds were shifted from the heated space to start the process of solidification. At the end the ceramic molds

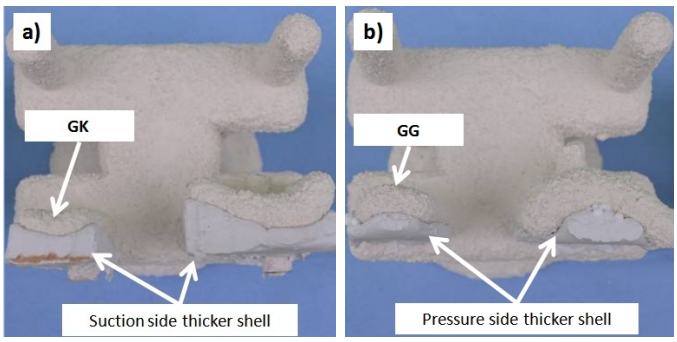

Fig. 2. Pattern assemblies with thicker ceramic layer: a) on the suction side, b) on the pressure side of the airfoil

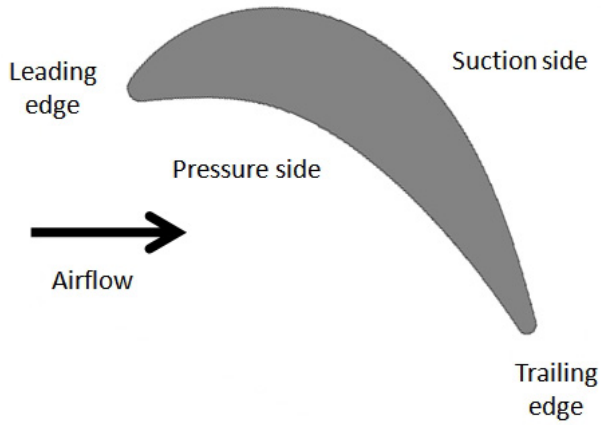

Fig. 3. The suction and pressure side of the airfoil

were broken and final castings were cut off. Two selected for the microstructural investigations castings (GK and GG) were cut in the way presented in Fig. 4.

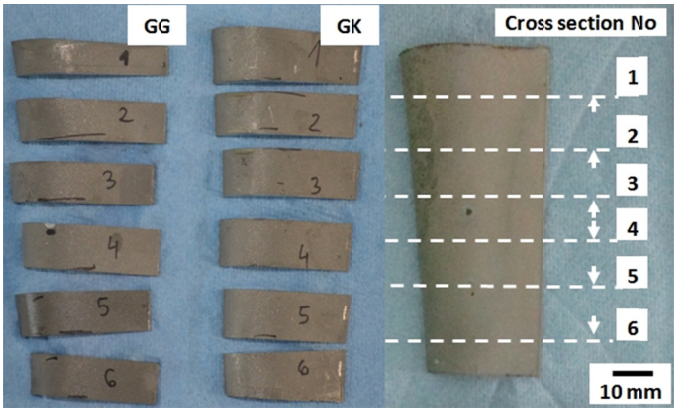

Fig. 4. The final cross-sections for the investigation and the cast with marked the way of cutting

The cross-sections were included and prepared according to traditional scheme of sample preparation for nickel-based superalloys (grinding and polishing). To reveal the microstructure of the investigated material the surfaces of the samples were etched in a mixture of 100 ml H_2O, 100 ml HCl, 100 ml HNO_3 and 3 g MoO_3. The microstructural investigations of the cross-sections of the castings (GK and GG) were carried out by means of Hitachi

S-4200 scanning electron microscope. The recorded microphotographs were next applied for computer-aided image analysis by means of Met-Ilo program to estimate quantitatively the main parameters describing the ($\gamma + \gamma'$) eutectic islands occurring in the investigated superalloy. Finally, the obtained results of the measurements of the ($\gamma + \gamma'$) eutectic islands were analysed in accordance to the typical statistical methodology. The amount of ($\gamma + \gamma'$) eutectic in Ni-based superalloys affect the properties, that is why its evaluation is so important. As an example one can cite the result of the research on MAR-M247 superalloy which confirmed that the room temperature yield strength increased and the ductility decreased as the amount of ($\gamma + \gamma'$) eutectic was reduced [9]. Furthermore, in as-cast alloys with a high volume fraction of ($\gamma + \gamma'$) eutectic, the complete dissolution of γ' by the appropriate heat treatment is of extreme importance [10].

4. Results

Thanks to the accepted way of cutting of the airfoils one can be able to observe and confirm with the measurements if the two options of ceramic layer putting on during investment casting process influence the solidification conditions and appearing ($\gamma + \gamma'$) eutectic islands as well as if there is diversification of morphology, size and shape of ($\gamma + \gamma'$) eutectic at height of the aerofoil of the blade.

The various eutectic 2D structures visible on the images (Fig. 5) result from the different observation plane and their distance from the fine γ/γ' centre. Graphical 3D illustration of the parent eutectic starting with a fine γ/γ' structure in the centre, the spatial expansion changes into a coarsening finger-shaped γ' with small γ channels, what is described in the work [11].

The ($\gamma + \gamma'$) eutectic islands were observed in the analyzed material in the interdendritic spaces.

Precise quantitative evaluation of ($\gamma + \gamma'$) eutectic islands is complicated because of their complex morphology. It requires image processing and mathematical transformations to obtain binary image of ($\gamma + \gamma'$) eutectic areas to measurements. The example of detection of ($\gamma + \gamma'$) eutectic islands was presented in Fig. 6.

The measurements of ($\gamma + \gamma'$) eutectic areas were performed on the binary images with detected ($\gamma + \gamma'$) eutectic. The results of the measurements were presented in Tables 1 and 2.

TABLE 1

The results of the measurements of ($\gamma + \gamma'$) eutectic areas on the cross-sections of the GG casting

Sample	A_A [%]	$v(A_A)$ [%]	$\bar{A}$ [µm^2]	$v(\bar{A})$ [%]
GG1	0.782	109.9	34.45	123.5
GG2	0.788	109.1	21.96	119.2
GG3	1.405	61.73	23.98	125.8
GG4	1.475	106.1	26.85	123.2
GG5	1.117	77.96	25.10	132.7
GG6	1.093	83.61	24.46	108.1

TABLE 2

The results of the measurements of ($\gamma + \gamma'$) eutectic areas on the cross-sections of the GK casting

Sample	A_A [%]	$v(A_A)$ [%]	$\bar{A}$ [µm^2]	$v(\bar{A})$ [%]
GK1	0.803	105.0	15.66	138.1
GK2	0.821	80.81	14.37	150.6
GK3	1.425	144.0	17.06	164.6
GK4	1.283	67.49	27.38	125.0
GK5	1.202	53.65	20.51	100.3
GK6	1.123	79.37	23.24	104.4

A_A – area fraction, $v(A_A)$ – coefficient of variation of area fraction, $\bar{A}$ – mean plane section area, $v(\bar{A})$ – coefficient of variation of mean flat surface

The attention was focused on two parameters describing the ($\gamma + \gamma'$) eutectic islands: A_A – area fraction and $\bar{A}$ – mean plane section area. The presented data were used for one-way and two-way analysis of variance (abbreviated ANOVA). It is a technique used to compare in statistics means of two or more samples (using Fisher-Snedecor distribution). The obtained results were the following: you can observe that there is a lack of significant difference between cross sections of GG cast (p value equals 0.34) and similarly GK cast (p value equals 0.61) – see Figs. 7 and 8.

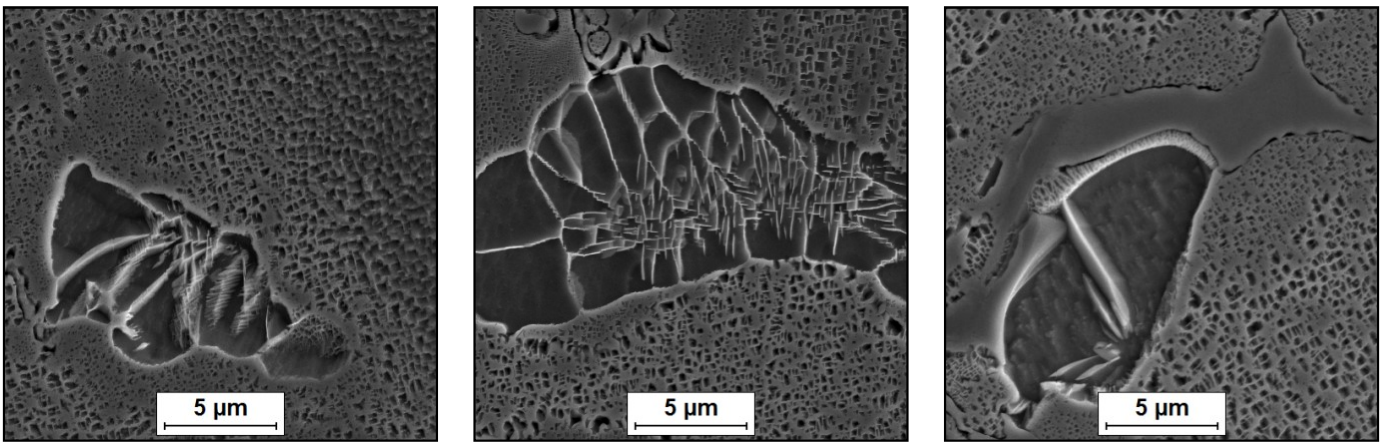

Fig. 5. The microstructure of the IN 713C superalloy with the ($\gamma + \gamma'$) eutectic islands

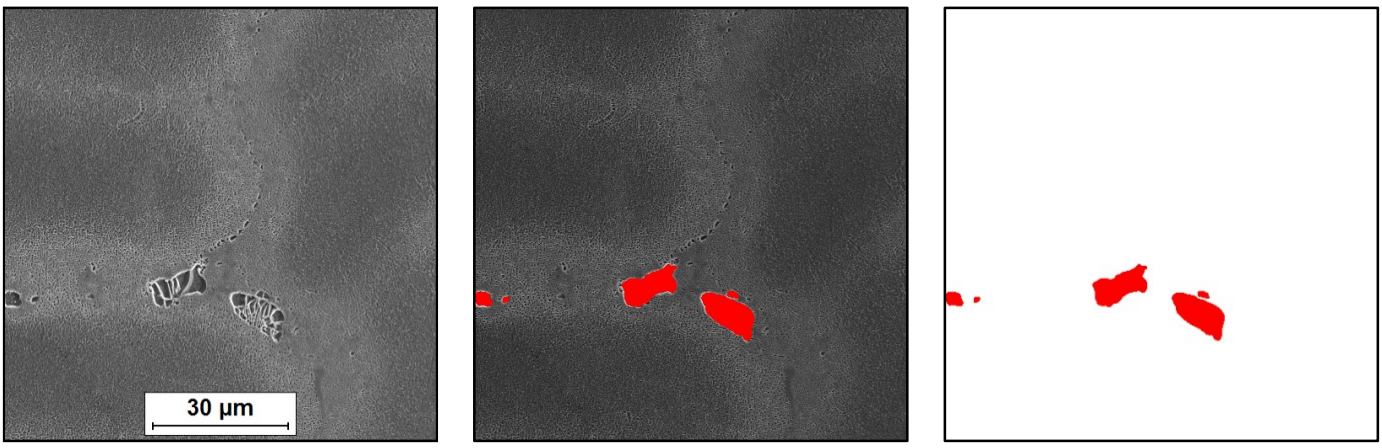

Grey image | Binary image on the grey image | Binary image of ($\gamma + \gamma'$) eutectic areas

Fig. 6. Example of image processing with detection of ($\gamma + \gamma'$) eutectic areas

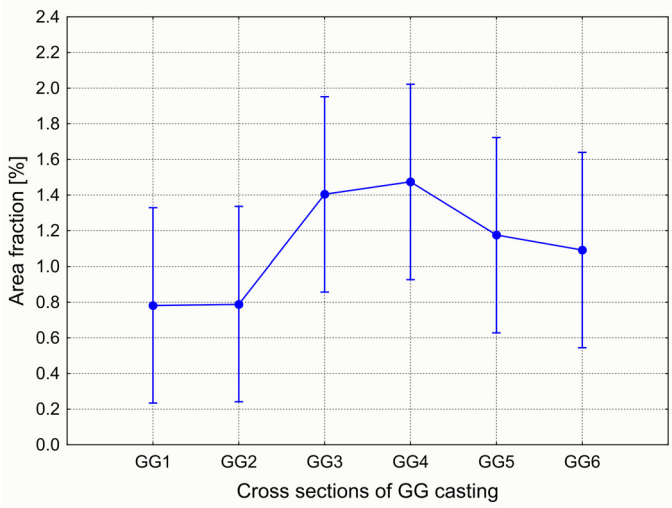

F(5, 84) = 1.1483; p = 0.34161

Fig. 7. Comparison of area fraction of ($\gamma + \gamma'$) eutectic areas on the cross sections of GG cast

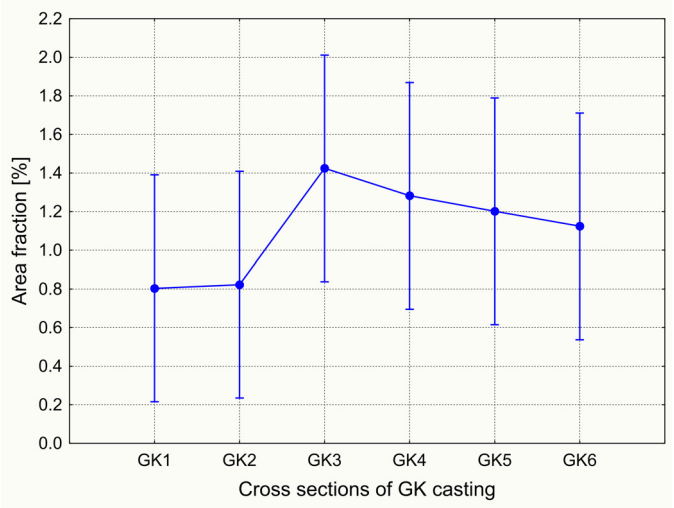

F(5, 84) = 0.072117; p = 0.60937

Fig. 8. Comparison of area fraction of ($\gamma + \gamma'$) eutectic areas on the cross sections of GK cast

Vertical segments (Figs. 7÷16) indicate the confidence intervals for value 0.95. For all analyses a significance level was assumed 0.05.

Taking into consideration comparison between conditions of two technologies (GG and GK cast) the results of the area fraction of ($\gamma + \gamma'$) eutectic areas show that if we expect a similar mean value of area fraction, there is lack of significant difference between cross-sections comparing together both technologies (p value equals 0.95) – Fig. 9. But if we compare jointly the cross-sections from GG cast with the cross-sections from GK cast some differentiation starts to be visible (p value equals 0.11) while there is still a lack of significant difference statistically – Fig. 10.

The second analyzed parameter describing ($\gamma + \gamma'$) eutectic areas is a mean plane section area. In Figs. 11 and 12 the results of ANOVA tests with plane sections area were presented. In the case of GG cast there is a lack of significant difference between the cross-sections (p value equals 0.63), but there is a significant difference between the cross-sections of GK cast (p value equals 0.02).

Comparing jointly two technologies (GG and GK cast) one can observe that there is very significant difference between mean plane section area of ($\gamma + \gamma'$) eutectic areas because p value equals 0.005 (Fig. 13). There is a lack of significant difference statistically between the cross-sections of two casts GG and GK comparing them together (p value equals 0.17), but some differentiation starts to be visible – Fig. 14.

If we would like to find the answer for the question if there is an interaction between technology (GK and GG cast) and cross-sections of the cast taking into consideration mean plane section area of ($\gamma + \gamma'$) eutectic areas, we could use the results from the ANOVA method showed in Fig. 15 and 16.

There is no significant interaction between the technology and cross-sections of the casts (p value equals 0.2). The most

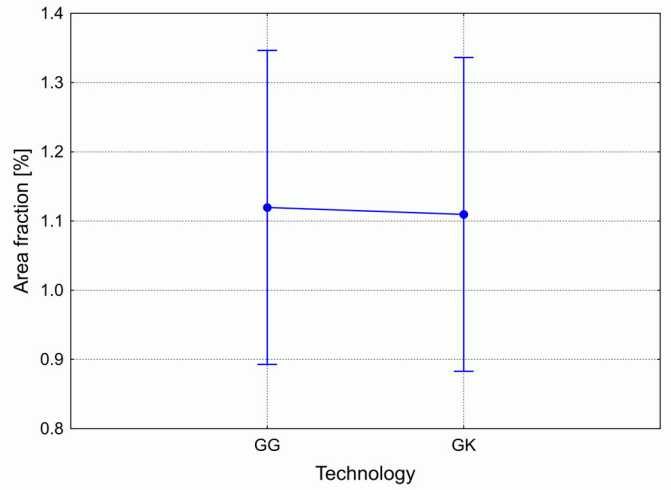

F(1, 173) = 0.00379; p = 0.95100

Fig. 9. Comparison of area fraction of ($\gamma + \gamma'$) eutectic areas in regard to conditions of two technologies (GG and GK)

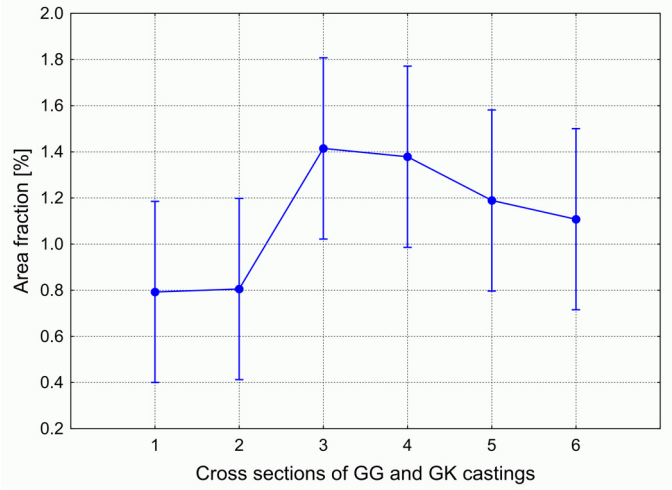

F(5, 173) = 1.8407; p = 0.10731

Fig. 10. Comparison of area fraction of ($\gamma + \gamma'$) eutectic areas between the cross sections of GK and GG cast jointly

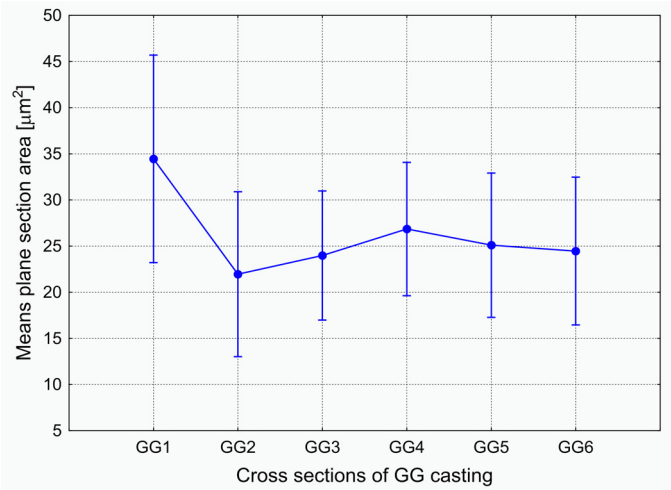

F(5, 354) = 0.69108; p = 0.63049

Fig. 11. Comparison of mean plane section area of ($\gamma + \gamma'$) eutectic areas on the cross sections of GG cast

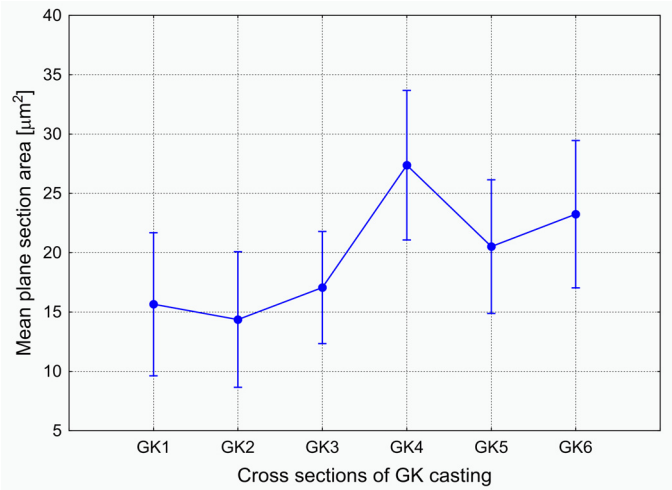

F(5, 466) = 2.6471; p = 0.02252

Fig. 12. Comparison of mean plane section area of ($\gamma + \gamma'$) eutectic areas on the cross sections of GK cast

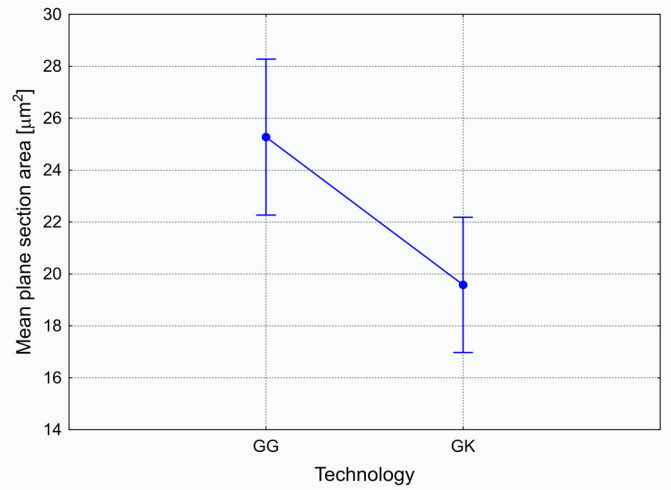

F(1, 825) = 7.9932; p = p = 0.00481

Fig. 13. Comparison of mean plane section area of ($\gamma + \gamma'$) eutectic areas in regard to conditions of two technologies (GG and GK)

F(5, 825) = 1.5572; p = 0.16976

Fig. 14. Comparison of mean plane section area of ($\gamma + \gamma'$)eutectic areas between the cross sections of GK and GG cast jointly

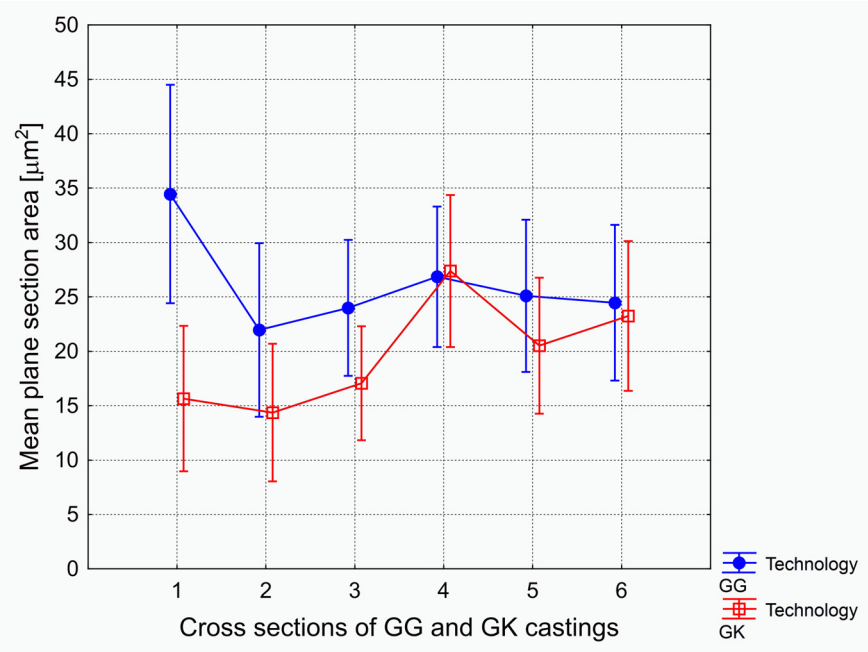

$F(5, 820) = 1.4496; \quad p = 0.20412$

Fig. 15. Comparison of both technologies with the cross sections of GK and GG cast jointly in regard to mean plane section area of ($\gamma + \gamma'$) eutectic areas

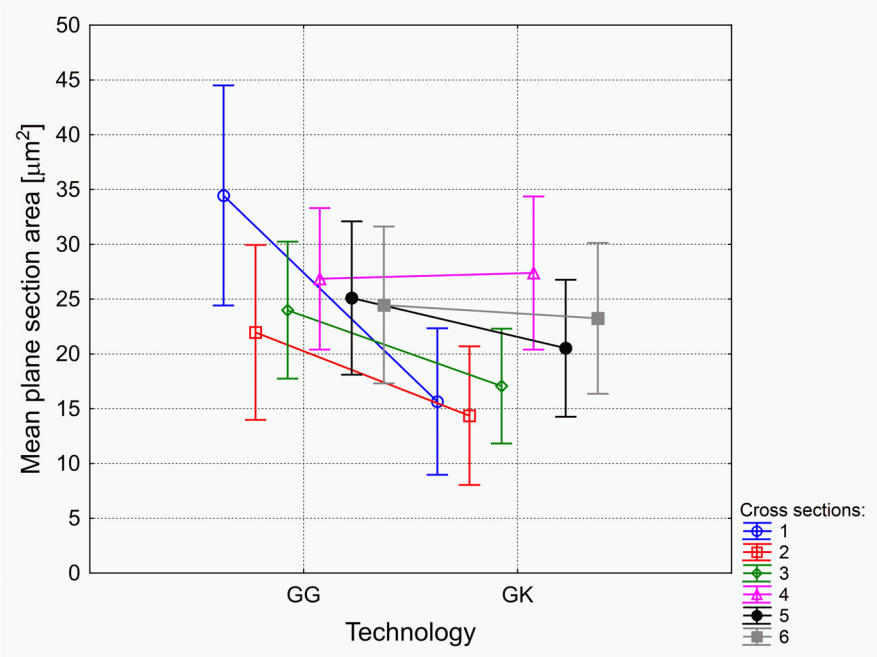

$F(5, 820) = 1.4496; \quad p = 0.20412$

Fig. 16. Comparison of both technologies and the six cross sections of GK and GG casts in regard to mean plane section area of ($\gamma + \gamma'$) eutectic areas between

visible divergence occurrs in the case of the cross-section No. 1 what is probably connected with the unlike conditions of heat transfer and local solidification conditions as the rest of the cross-sections.

4. Summary and conclusions

The observations of the microstructure on the all cross-sections of the investigated elements and the performed statistical analyses of occurring of ($\gamma + \gamma'$) eutectic areas in the material enabled to determine diversification or a lack of diversification of the microstructure. The size, distribution, morphology and

orientation of microstructural constituents depends strongly on local solidification conditions. A significant diversification of microstructure at the height of the whole cast could indicate a necessity of a further improvement of a technological process especially connected with a heterogeneous thickness of a multilayer ceramic moulds.

Based on the carried out investigations the following conclusions can be made:

1. The presented results show that evaluation the $(\gamma + \gamma')$ eutectic areas in the analyzed casts from IN 713C superalloy is possible using by image analysis.
2. The analysis of repeatability of technology was carried on by means of statistical ANOVA methods.
3. Analysis of the microstructure of the IN 713C material requires knowledge and experience. Only application of complex procedure of quantitative description of material microstructure can give good and repeatable results.
4. The conducted comparison between two technological options of shell mould deposition showed that:
   a) there is a lack of significant difference between GG and GK cross-sections considering together and separately taking into consideration area fraction of $(\gamma + \gamma')$ eutectic,
   b) there are visible divergence between GG and GK cross-sections taking into consideration mean plane section area of $(\gamma + \gamma')$ eutectic.
5. Thicker deposition of the ceramic layer on the suction side of aerofoil (GK cross sections) gives greater diversification of mean plane section area of $(\gamma + \gamma')$ eutectic than deposition on thicker layer on the pressure side.
6. The cross-section No. 1 characterizes the most deviation from the rest cross-sections in the case of mean plane section area of $(\gamma + \gamma')$ eutectic. It points that this area of aerofoil should be especially in control during deposition of ceramic layer.
7. It seems that one should use more sophisticated, but also more computationally expensive statistical non-parametric methods [12÷14] in further investigation to reveal relationships between factors deeper than it is possible in classic statistical analysis [1], however the computational cost of such enhancement is very high [15]. It may include specific non-parametric methods for the analysis of multidimensional sparse data [16-22], even with a multiphysics approach [23-25] and the fuzzy statistics [14].

The investment casting industry is developing. It improves casting quality and reduces manufacturing costs. Production of mould described here takes 24 hours. Depending of the used materials, added components and size of the component it can take 24 up to 72 hours. Drying and strength development are the most significant rate-limiting factors in reduction of time and costs of production. That is why the research on ceramic shells are so important for investment casting process. The number of coats applied to the wax pattern should be optimized, which would reduce the drying time, material costs and production time. The described in the work results could be usefull for optimization of shell thickness and could be applied for modeling using casting software like Procast, Quickcast, Solidcast, etc.

Acknowledgements

Authors would like acknowledgment support from The National Centre for Research and Development, project nr: INNOTECH-K2/IN2/8/181849/NCBR/13.

REFERENCES

[1] H. Pham (ed.), The Springer Handbook of Engineering Statistics, Springer, 2006.
[2] F.R. Sias Jr., Lost-Wax Casting: Old, New, and Inexpensive Methods, Woodsmere Press, Pendleton, 2006.
[3] J.E. Sopcak, Handbook of Lost Wax or Investment Casting, Gembooks, 1986.
[4] P.R. Beeley, R. F. Smart (eds.), Investment Casting, David Brown Book Company, 2008.
[5] S. Pattnaik, D.B. Karunakar, P.K. Jha, J. Mater. Process. Tech. 212, 2332-2348 (2012).
[6] S. Jones, C. Yuan, J. Mater. Process. Tech. **135,** 258-265 (2003).
[7] Y. Huang, L. Wang, Y. Liu, S. Fu, J. Wu, P. Yan, Trans. Nonferrous Met. Soc. China **21**, 2199-2204 (2011).
[8] J. Safari, S. Nategh, J. Mat. Proc. Technol. **176**, 240-250 (2006).
[9] K.L. Gasko, G.M. Janowski, B.J. Pletka, Mater. Sci. Eng.A 104, 1-8 (1988).
[10] L. Avala, Ch.V.S. Murthy, P.K. Singh, B. Chaitanya, S. Kumar, Int. J. Theoret. Appl. Res. Mechan. Eng. **2/4**, 2319-3182 (2013).
[11] A. Heckl, R. Rettig, S. Cenanovic, M. Göken, R.F. Singer, J. Cryst. Growth **312** 2137-2144 (2010).
[12] J. Pietraszek, E. Skrzypczak-Pietraszek, Adv. Mat. Res. **874**, 151-155.
[13] R. Ulewicz, J. Balk. Tribol. Assoc. **21**, 166-172.
[14] J. Pietraszek, M. Kolomycki, A. Szczotok, R. Dwornicka, in: N.T. Nguyen, Y. Manolopoulos, L. Iliadis, B. Trawinski (Eds.), 8th International Conference on Computational Collective Intelligence, (ICCCI), Pt I, 260-268 (2016).
[15] A.B. Owen, Empirical Likelihood, Chapman & Hall/CRC, Boca Raton, 2001.
[16] J. Pietraszek, 6th International Conference on Neural Networks and Soft Computing, 2003, 250-255.
[17] E. Skrzypczak-Pietraszek, A. Hensel, Pharmazie **55**, 768-771 (2000).
[18] A. Szczotok, Materialwiss. Werkst. **46**, 320-329 (2015).
[19] L. Skrzypczak, E. Skrzypczak-Pietraszek, E. Lamer-Zarawska, B. Hojden, Acta Soc. Bot. Pol. **63**, 173-177 (1994).
[20] N. Radek, A. Sladek, J. Broncek, I. Bilska, A. Szczotok, Adv. Mater. Res. **874**, 101-106 (2014).
[21] I. Dominik, J. Kwasniewski, K. Lalik, R. Dwornicka, 32nd Chin. Contr.Conf., 2013, 7505-7509.
[22] R. Dwornicka, Adv. Mater. Res.-Switz. **874**, 63-69 (2014).
[23] T. Styrylska, J. Pietraszek, Z. Angew. Math. Mech. **72**, T537-T539 (1992).
[24] A. Tiziani, A. Molinari, J. Kazior, G. Straffelini, Powder Metall. Int. **22**, 17-19 (1990).
[25] F. Deflorian, L. Ciaghi, J. Kazior, Werkst. Korros. **43**, 447-452 (1992).